# Size-, Composition- and Shape-Dependent Toxicological Impact of Metal Oxide Nanoparticles and Carbon Nanotubes toward Bacteria

ANGÉLIQUE SIMON-DECKERS,[†] SYLVAIN LOO,[†] MARTINE MAYNE-L'HERMITE,[‡] NATHALIE HERLIN-BOIME,[‡] NICOLAS MENGUY,[§] CÉCILE REYNAUD,[‡] BARBARA GOUGET,[†,∥] AND MARIE CARRIERE*,[†]

*CEA, IRAMIS, Service interdisciplinaire des systèmes moléculaires et matériaux (CEA-CNRS UMR9956) CEA Saclay, 91191 Gif sur Yvette, France, CEA, IRAMIS, SPAM, Laboratoire Francis Perrin (CEA-CNRS URA2453) Gif sur Yvette, France, and IMPMC, UMR 7590 CNRS, Université Pierre et Marie Curie, Université Paris Diderot, IPGP, 140 rue de Lourmel 75015 Paris, France*

*Received June 9, 2009. Revised manuscript received September 21, 2009. Accepted September 22, 2009.*

Ecotoxicological effects of nanoparticles (NP) are still poorly documented while their commercialization for industrial and household applications increases. The aim of this study was to evaluate the influence of physicochemical characteristics on metal oxide NP and carbon nanotubes toxicological effects toward bacteria. Two strains of bacteria, *Cupriavidus metallidurans* CH34 and *Escherichia coli* MG1655 were exposed to $TiO_2$ or $Al_2O_3$ NP or to multiwalled-carbon nanotubes (MWCNT). Particular attention was paid on optimizing NP dispersion to obtain nonagglomerated suspensions. Our results show that NP toxicity depends on their chemical composition, size, surface charge, and shape but not on their crystalline phase. MWCNT toxicity does not depend on their purity. Toxicity also depends on the bacterial strain: *E. coli* MG1655 is sensitive to NP, whereas *C. metallidurans* CH34 is not. Interestingly, NP are accumulated in both bacterial strains, and association between NP and bacteria is necessary for bacterial death to occur. NP may then represent a danger for the environment, causing the disappearance of some sensitive bacterial strains such as *E. coli* MG1655, but also being mobilized by nonsensitive strains such as *C. metallidurans* CH34 and transported through the whole ecosystem.

## Introduction

Assessing the risk of manufactured nanoparticles toward the environment requires the knowledge of their fate after release, i.e., their mobility, reactivity and persistence in environmental compartments, but also their impact on living organisms.

The interaction of metal oxide NP with bacteria has already been demonstrated (*1*−*12*), sometimes leading to a loss of viability. Little is known about the mechanisms underlying this effect, in some studies it was related to NP penetration through bacterial cell wall (*3, 5, 10, 11*), and/or to the redox activity of NP (*2*). It is known that the size, shape and crystalline structure of NP affect their toxicological impact on eukaryotic cells (*13*). This relationship has also been described on bacteria with silver NP: 1−10 nm Ag NP present greater impact on bacteria than larger particles (*14*), and triangular-shaped Ag NP display greater biocidal action than rod or spherical-shaped ones (*15*). The smallest ZnO nanoparticles are also the most bactericidal (*8*), but such effect was not detected with $TiO_2$ (*1*).

Single- and multiwalled carbon nanotubes (SWCNT and MWCNT, respectively), were bactericidal to *E. coli*, and it was linked to bacterial attachment to aggregates of nanotubes (*16*−*18*). SWCNT are more toxic than MWCNT, suggesting that the diameter plays a role in bactericidal effect (*16*). On eukaryotic cells, a correlation has been made between the toxicological effects of CNT and the presence of metal-based impurities (*19*).

Up to now, no comprehensive study has made any relationship between metal oxide NP chemical composition, size, shape, crystalline structure, and their toxicological effects and ad- or absorption with bacteria. Neither was made any relationship between the presence of metal-based impurities in nanotubes and their toxicity toward bacteria. To address these question, a potentially sensitive bacterial strain (*E. coli* MG1655), and an environmentally relevant bacterium, resistant to many metallic pollutants, *C. metallidurans* CH34 (*20, 21*), were exposed to various NP. Bacteria were exposed to various $TiO_2$, $Al_2O_3$ NP, or MWCNT, since these NP are or will soon be the most produced NP and consequently the most potentially released in the environment. A special emphasis was put on the preparation of well dispersed NP suspensions for bacterial exposure. Our results enable to draw a correlation between physicochemical characteristics, antibacterial properties, and bacterial internalization, which proves that characterization of NP physicochemical parameters, as precise as possible, is a prerequisite for the proper assessment of their toxicological effects.

## Material and Methods

**Nanoparticles (NP).** MWCNT were prepared by aerosol-assisted catalytic chemical vapor deposition (CVD) using Fe as catalyst (*22*) and heat purified (*23*) to reduce the 4.24 wt.% Fe of raw MWCNT to 0.08 wt.% in annealed nanotubes. $TiO_2$-A12 and $TiO_2$-R20 NP were synthesized by laser pyrolysis (*24*), and annealed under air. $TiO_2$-A25 (AEROXIDE P25) and $Al_2O_3$ (AEROXIDE AluC) were from Degussa; $TiO_2$-R9 (ref 637262), $TiO_2$-R700 (ref 224227), $TiO_2$-A17 (ref 637254) and $TiO_2$-A140 (ref T8141) were from Sigma-Aldrich. In the denomination of $TiO_2$ NP, A is for anatase, R for rutile; and the number gives the mean diameter of NP. Suspensions were prepared in ultrapure sterile water by pulsed sonication, 30 mn at 4 °C. Gum Arabic (0.25 wt.%) was added as a dispersing agent to MWCNT.

**Characterization of NP.** The characteristics of NP are summarized in Table 1 and in (*25*). Specific surface areas (SSA, $m^2/g$) were measured using Brunauer, Emmet and Teller (BET) method (*26*). BET diameter ($D$, nm) of spherical NP was calculated as $D = 6/(\rho \times \mathrm{SSA})$, taken density (g/

* Corresponding author phone: +33169085235; fax: +33169086923; e-mail: marie.carriere@cea.fr.
[†] Service interdisciplinaire des systèmes moléculaires et matériaux.
[‡] Laboratoire Francis Perrin.
[§] Université Pierre et Marie Curie, Université Paris Diderot.
[∥] Present address: AFSSA, Scientific Department, 27/31 avenue du Général Leclerc, 94701 Maisons-Alfort, France.

10.1021/es9016975 CCC: $40.75 
Published on Web 10/07/2009

**TABLE 1. Nanoparticles Physico-Chemical Characteristics[a]**

| | supplier | morphology | size (TEM) | SSA ($m^2$ /g) | size (BET) | $\zeta$ (mV) | PZC | crystalline structure |
|---|---|---|---|---|---|---|---|---|
| $Al_2O_3$ | Degussa | spherical | 11 nm (13 nm) | 83 (100 ± 15) | 18 | 120 | 8.4 | |
| $TiO_2$-A25 | Degussa | spherical | 25 nm (21 nm) | 46 (50 ± 15) | 33 | 44 | 7 | 86% anatase |
| $TiO_2$-A12 | CEA | spherical | 12 nm | 82 | 19 | 20 | 6.4 | 95% anatase |
| $TiO_2$-A17 | Sigma | spherical | 17 nm | 122 | 12 | 12 | 5.6 | 100% anatase |
| $TiO_2$-A140 | Sigma | spherical | 142 nm (<44 $\mu$m) | 10 | 152 | −33 | 5.2 | 100% anatase |
| TiO2-R20 | CEA | spherical | 21 nm | 73 | 23 | 0 | | 90% rutile |
| $TiO_2$-R9 | Sigma | elongated | *L*: 68 nm (<100 nm)<br>*D*: 9 nm | 118 ± 1 | | −50 | | 100% rutile |
| $TiO_2$-R700 | Sigma | spherical | 707 nm | 2 ± 0 | 707 | 1 | 5.4 | 96% rutile |
| MWCNT | CEA | elongated | *L*: 1.5 $\mu$m<br>*D*: 44.0 nm | 42 ± 2 | | | | |

[a] Size was either measured by TEM observation (size TEM) or deduced by calculation from SSA data (size BET). SSA was measured according to BET protocol. Italic indications are the theoretical values given by suppliers. Zeta potential ($\zeta$) was measured in ultrapure water (pH 5.5). PZC: point of zero charge, obtained from $\zeta$ measurement as a function of pH. Crystal structure was deduced from XRD diagram. *L*: length, *D*: diameter.

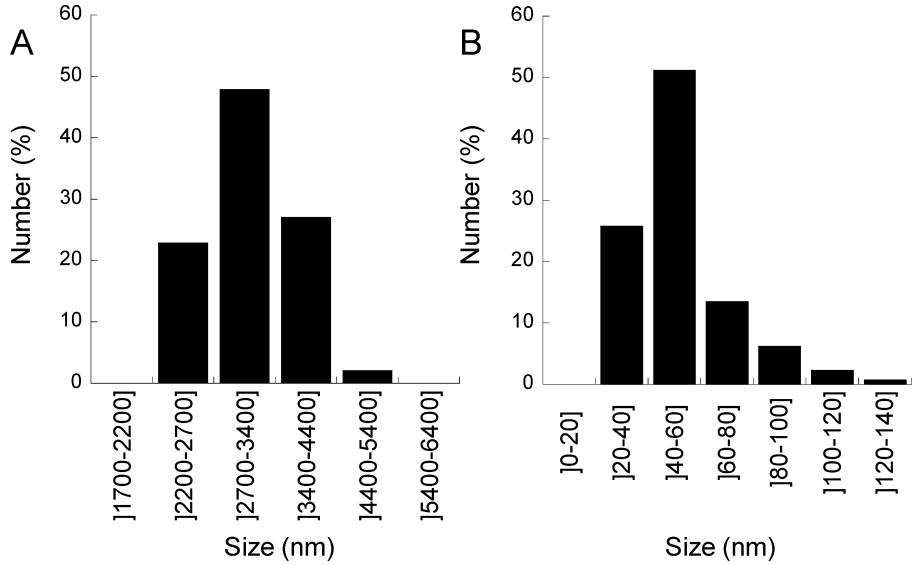


**FIGURE 1. Nanoparticles agglomeration in exposure media. The hydrodynamic diameter of $TiO_2$-A25 was determined by photon correlation spectroscopy after dispersion by sonication in water and then dilution in TSM medium (A) or in water (B). Results are expressed in number.**

$cm^3$) as $\rho = 3.90$ (anatase $TiO_2$) and 3.99 ($Al_2O_3$). Shape, diameter, and length of NP and MWCNT were determined by transmission electron microscopy (TEM), using a Philips EM208 microscope at 80 kV, and optical microscopy (×40), on 150−200 NP and MWCNT, randomly chosen. The hydrodynamic diameters and zeta potentials were measured on a ZetaSizer 3000HS (Malvern, Worcestershire, UK) by photon correlation spectroscopy (PCS) and zetametry. The pH value at their zero point of charge (PZC) was obtained from their zeta potential as function of pH, thanks to a MPT-1 titrator. Dissolution of Ti or Al ions from NP was determined by inductively coupled plasma mass spectrometry (ICP-MS) using a X7 series quadrupole (Thermo Electron corporation, Cergy-Pontoise, France).

**Bacterial Growth and Exposure.** Bacteria were grown aerobically under agitation. *Cupriavididus metallidurans* CH34, provided by Max Mergeay (SCK/CEN, Mol, Belgium) was grown at 29 °C in Tris Salt Mineral medium (TSM) with 1% gluconate as a carbon source, *Escherichia coli* MG1655 (*27*) at 37 °C in Luria−Bertani medium (LB). Bacteria were exposed to NP diluted in water, at room temperature under gentle stirring.

**Viability and Reactive Oxygen Species Assays.** NP impact on bacterial membrane integrity was assessed with the LIVE/DEAD BACLIGHT assay (Introvigen), following the manufacturer's instructions. This assay is based on the incorporation of propidium iodide (PI) in bacteria with damaged membranes and syto 9 in all bacteria. Syto 9/PI fluorescence ratio was determined and the percentage of dead cells was calculated from a calibration curve, obtained from bacteria exposed to isopropanol. Intracellular level of reactive oxygen species was monitored by following the fluorescence of 2′,7′-dichlorodihydrofluorescein diacetate acetyl ester (H2DCF-DA, Invitrogen). This cell-permeant indicator becomes fluorescent when cleaved by intracellular esterases and oxidized by $H_2O_2$, $ROO^{\bullet}$, $ONOO^{-}$. Detailed protocols are given in the Supporting Information (SI). Due to the photoreactivity of anatase $TiO_2$ NP, all experiments were performed in a dark room illuminated with an inactinic light and all containers were covered with aluminum foils.

**Transmission and Scanning Transmission Electron Microscopy (TEM and STEM).** After exposure, bacteria were fixed with 2.5% glutaraldehyde and postfixed with $OsO_4$, dehydrated in graded concentrations of ethanol and embedded in Epon resin. Ultrathin sections were cut and counterstained with Reynold's and uranyl acetate. Drops of bacteria exposed to MWCNT, dried onto a copper grid, were directly observed. Grids were observed on a CM 12 Philips TEM at 80 kV, or on a JEOL 2010F STEM at 200 kV, equipped with a field emission gun, a high-resolution UHR pole piece,

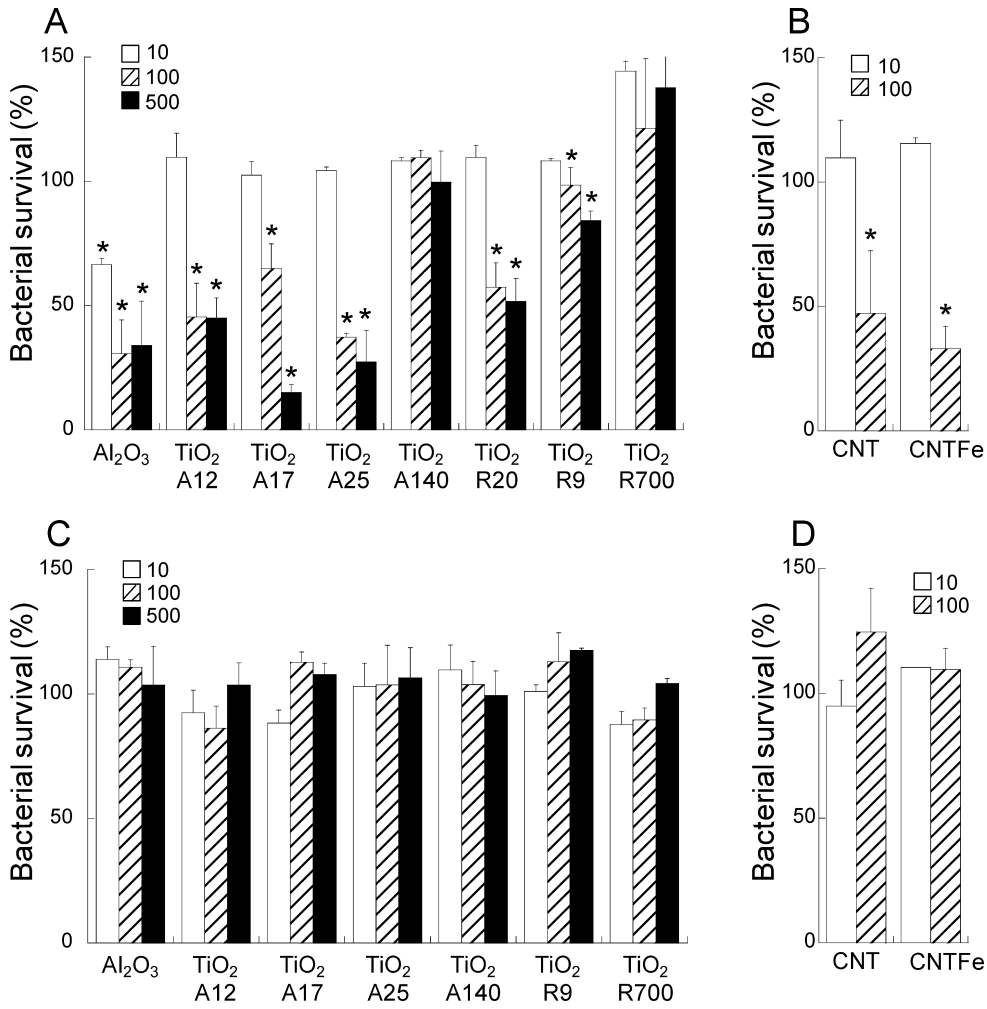


**FIGURE 2. Loss of viability induced by nanoparticle exposure. Cell death was evaluated using the live/dead baclight assay. *E. coli* MG1655 (A, B) and *C. metallidurans* CH34 (C, D) were exposed for 24 h to 10, 100, 500 mg/L of $TiO_2$ or $Al_2O_3$ nanoparticles (A, C) or to 10 or 100 mg/L of MWCNT (B, D) prepared as aqueous suspensions. Comparison with a positive control permitted to determine the percentage of bacterial viability. Statistical significance: *, $p < 0.05$.**

a Gatan energy filter GIF 100 and a X-ray energy dispersive spectrometer.

**Statistical Analysis.** Results are expressed as mean ± standard deviation of at least three assays. Statistical evaluation was performed with STATISTICA software. One-way Kruskal−Wallis ANOVA was used, followed by Mann−Whitney *u*-test. $p < 0.05$ was considered to be statistically significant (*).

## Results

**Effect of Nanoparticles on Bacterial Viability.** Bacteria were first exposed to NP suspensions diluted in culture medium and growth curves were drawn. No effect of NP was observed on the growth of C. *metallidurans* CH34 and *E. coli* MG1655 (not shown). In this condition the average hydrodynamic diameter of NP ranged between 2 and 4 $\mu$m (Figure 1A), meaning that NP were agglomerated. Agglomeration may avoid direct interaction of NP with bacteria. For this reason, we chose to perform next exposures with water-dispersed NP. When prepared in water, NP average hydrodynamic diameter was close to primary NP (TEM measurement), i.e., 25−140 nm (Figure 1B). However, just after exposure of bacteria to water-dispersed NP, eye-observation revealed agglomeration of NP together with bacteria. If plated on solid LB-agar, one bacteria/NP cluster, and not one bacterium would lead to the development of one colony. This classical method used to assess bacterial viability was thus irrelevant to evaluate the toxicity of NP. Consequently the fluorescence-based live/dead BACLIGHT assay was chosen to assess NP bactericidal activity, by means of membrane integrity assessment (Figure 2).

First *E. coli* MG1655 was exposed to NP. Significant loss of viability was observed after exposure to the smallest $TiO_2$ NP, whose diameter ranged from 10 to 25 nm: $TiO_2$-A12, -A17, -A25, and -R20 (Figure 2A). Decrease of bacterial viability was NP concentration-dependent, and reached 45, 15, 27, and 52%, respectively, of viable bacteria as compared to nonexposed bacteria, after a 24 h exposure to 100 mg/L of NP. In contrast, larger NP ($TiO_2$-A140 and -R700) had no effect on bacterial viability. Size-effect of NP has previously been described with ZnO NP (*7, 8*). Conversely, several studies showed either a size-independent bactericidal effect of $TiO_2$ NP (*1*), or no bactericidal effect (*4, 6*). However in these studies agglomeration of NP was not strictly controlled, contrary to our exposure conditions. Agglomeration may avoid direct association of NP with bacteria, thus avoiding cell wall penetration or membrane damage.

We show here that both anatase (A) and rutile (R) NP with mean diameter <25 nm induced comparable amounts of cell death, meaning that the crystalline phase of $TiO_2$ NP did not govern their toxicity. Anatase NP are assumed to be more toxic than rutile because of their photocatalytic properties when illuminated (*28*). Our experiments were performed in the dark, explaining that they do not show any overtoxicity

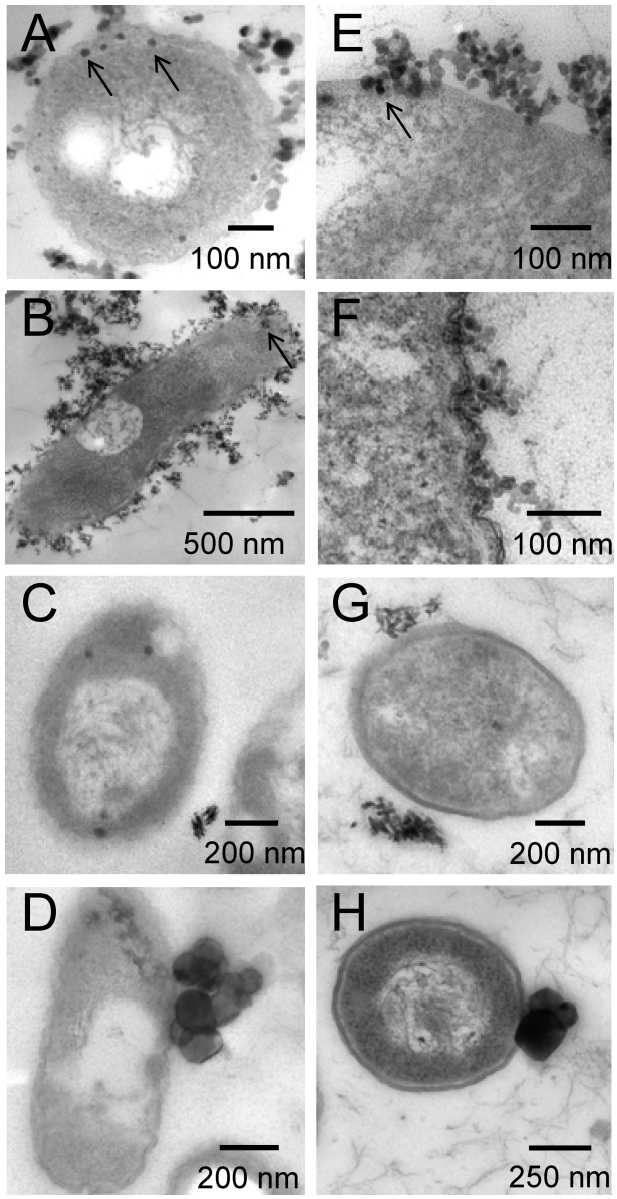


**FIGURE 3. Transmission electron microscopic observation of nanoparticles absorption in bacteria. *C. metallidurans* CH34 (A−D) and *E. coli* MG1655 (E−H) were exposed in ultrapure water for 24 h to 50 mg/L of $TiO_2$-A12 (A, E), $Al_2O_3$ (B, F), $TiO_2$-R9 (C, G), $TiO_2$-A140 (D, H).**

of anatase NP. We demonstrate here that, in the dark, rutile NP are as toxic as anatase NP, which confirms that, as proposed by Adams et al. (*1*), $TiO_2$ toxicity is not only driven by their photocatalytic properties, and that another mechanism leads to bacterial death even in the dark.

Among the $TiO_2$ NP tested in this study, and considering that NP with diameter <25 nm are toxic whatever their crystalline phase, $TiO_2$-R9 may be bactericidal. It was not the case. $TiO_2$-R9 is elongated-shaped and bears a negative zeta potential. Shape-dependent toxicological effect have already been described with ZnO NP (*8*), rod-shaped NP being less antibacterial than spherical NP. Our study confirms this assumption for $TiO_2$ NP.

Another point is that only NP having highly positive or neutral zeta potentials, i.e. $TiO_2$-A12, -A17, -A25, and -R20 were bactericidal, whereas NP having negative zeta potentials ($TiO_2$-R9 and -A140) did not. Indeed, electrostatic repulsion between negatively charged NP and the negatively charged cell surface of *E. coli* MG1655 may avoid association between bacteria and NP, and consequently limit their toxicity. Adsorption of NP to bacterial surface is thus a prerequisite for bactericidal effects to be observed.

$Al_2O_3$ NP induced a significant loss of viability on *E. coli* MG1655, appearing at lower concentrations relatively to $TiO_2$ NP. This result is in accordance with previously published data (*6, 7*). Furthermore, dissolved Al was measured by ICP-MS in the supernatant of $Al_2O_3$ NP suspension; it reached 14 mg/L, i.e., ca. 0.3% of the total amount of Al in the NP suspension. These Al ions may be partly responsible for $Al_2O_3$ NP bactericidal effect. Conversely, no Ti was detected in the supernatant of $TiO_2$ NP suspension.

Raw (CNTFe) or purified (CNT) MWCNT were bactericidal to *E. coli* MG1655 (Figure 2B): whatever their purity, they induced a 50−60% loss of viability (exposure 24 h at 100 mg/L). The absence of impact of metal impurities is probably due to their distribution in CNT: it is mainly located inside the tubes (*22*), and may then not directly interact with bacteria. Moreover CNT are generally purified by an acid-treatment (*16−18, 29, 30*). This treatment may modify the surface chemistry of purified MWCNT (*31*), generating structural defects which render them more reactive than raw MWCNT and consequently potentially more toxic to living organisms. In the present study, CNT were heat-treated, which limits surface modification and therefore reactivity.

Finally, the impact of NP or MWCNT exposure was evaluated on *C. metallidurans* CH34, known to be resistant to environmental stresses, particularly to survive in metal-contaminated biotopes (*21*). This bacterium was highly resistant to NP and MWCNT (Figure 2C and D). Resistance of *C. metallidurans* CH34 to metal is a complex process, involving efflux systems which detoxify the periplasm and cytoplasm by export of metal ions (*32*). An explanation to its resistance to NP and MWCNT may be that efflux systems are also able to export NP. However these systems are dedicated to ions, and are probably not able to transport large cargoes such as NP.

**Association of Nanoparticles with Bacteria.** To find an explanation to *E. coli* MG1655 sensitivity to NP and to the resistance of *C. metallidurans* CH34, the distribution of NP was characterized by TEM observation of exposed-bacteria thin sections. $TiO_2$-A12 and $Al_2O_3$ NP were adsorbed onto bacterial surface and localized in the periplasmic compartment of both *C. metallidurans* CH34 and *E. coli* MG1655 (Figure 3A, B, E, arrows). Conversely, $TiO_2$-R9 and $TiO_2$-A140 were not observed in the periplasm of bacteria (Figure 3C, D, G, and H). Scanning transmission electron microscopy coupled to energy dispersive spectroscopy, confirmed that the granules observed by TEM were Al-containing (Figure 4A and B) and Ti-containing clusters (Figure 4C and D), and thus probably $Al_2O_3$ or $TiO_2$ NP. Among the tested NP, the toxic ones were accumulated in bacterial periplasm, confirming that association between NP and bacteria is a prerequisite for the expression of their toxicity.

After exposure to MWCNT, due to their hardness it was not possible to prepare bacterial thin sections for TEM observation. Therefore, these bacteria were directly observed after deposition of a drop of suspension, dried on the TEM grid. Both bacteria adsorbed onto MWCNT (Figure 5A and B), but no evidence of MWCNT internalization was shown, even if bacterial wall was sometimes deeply invaginated by associated MWCNT (Figure 5C and D). In other studies (*16, 29*), it was demonstrated that carbon nanotubes damage bacterial membrane, leading to the release of cytoplasmic elements. This would need to be confirmed in our system.

Considering that $TiO_2$ and $Al_2O_3$ NP are internalized in both bacteria, the resistance of *C. metallidurans* CH34 relatively to *E. coli* MG 1655 cannot be explained by the efflux of NP from the periplasm of *C. metallidurans* CH34. Other hypothesis for this resistance may be the structure and

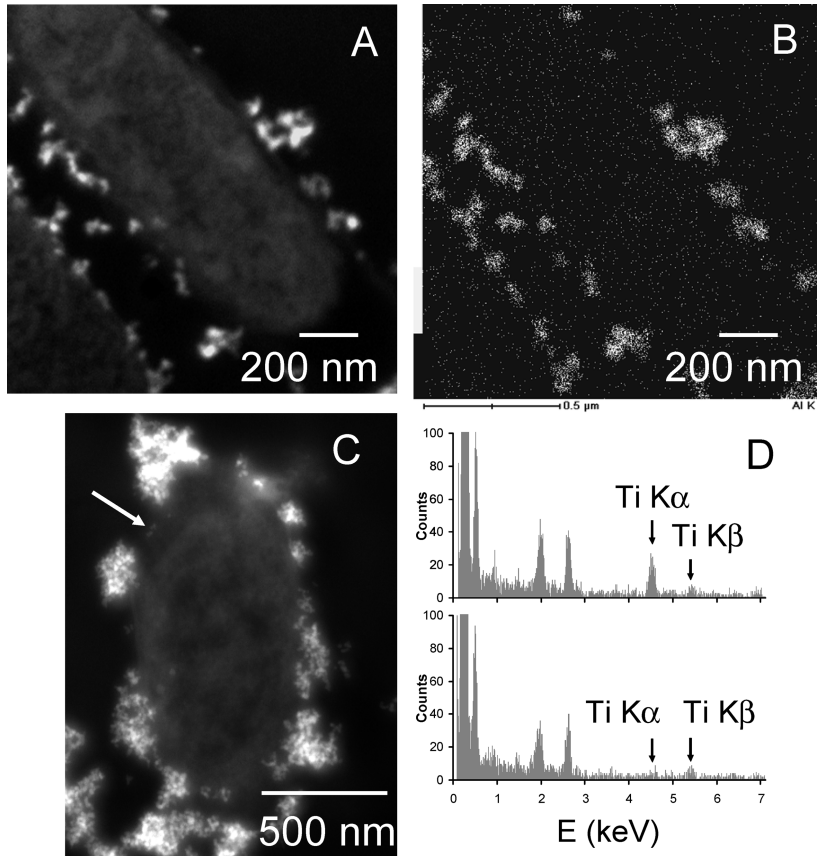


**FIGURE 4. Scanning transmission electron microscopy of bacteria exposed to nanoparticles, energy dispersive spectroscopic (EDS) analysis. *E. coli* MG1655 was exposed to 50 mg/L of $Al_2O_3$ (A, B) or $TiO_2$-A12 (C, D) for 24 h. Images allow to observe bacteria covered by electron dense nanoparticles (A, C). Distribution of Al observed by EDS imaging (B). EDS spectra (D, top) of an electron-dense granule (C, arrow) located in bacterial persiplasm or of the cytoplasm of the bacterium (D, bottom).**

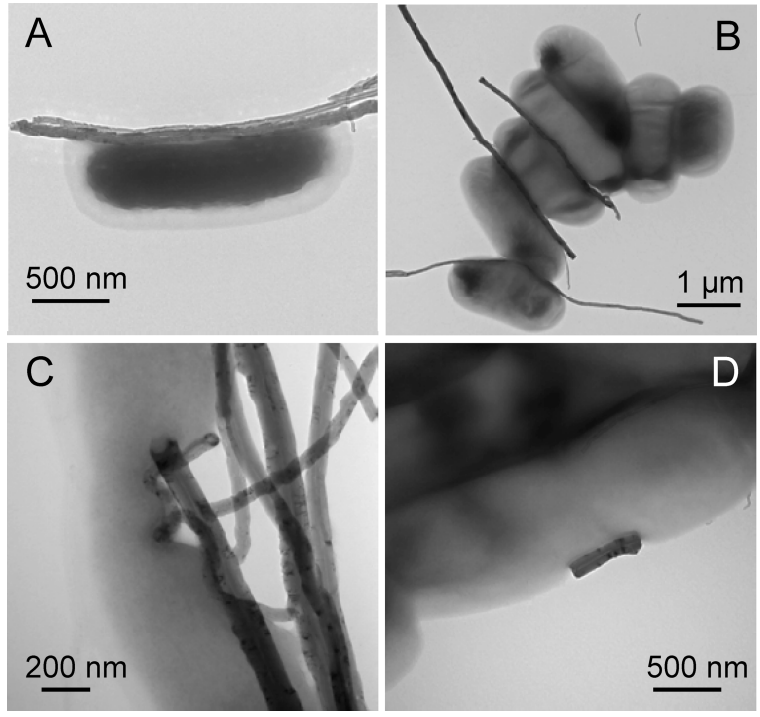


**FIGURE 5. Nanotube association with bacteria. *C. metallidurans* CH34 (A, C, D) or *E. coli* MG 1655 (B) were exposed for 24 h to 10 $\mu$g.ml$^{-1}$ of MWCNT in ultrapure water, and then directly observed by TEM.**

physical properties of their peptidoglycan (PG) layer (*33*), which may be more resistant in *C. metallidurans* CH34 than in *E. coli* MG 1655. NP transfer across the PG layer in *E. coli* MG1655 could enable their access to plasma membrane, leading to potential damage. Conversely, in *C. metallidurans* CH34, NP would be sequestered outside or in the PG layer

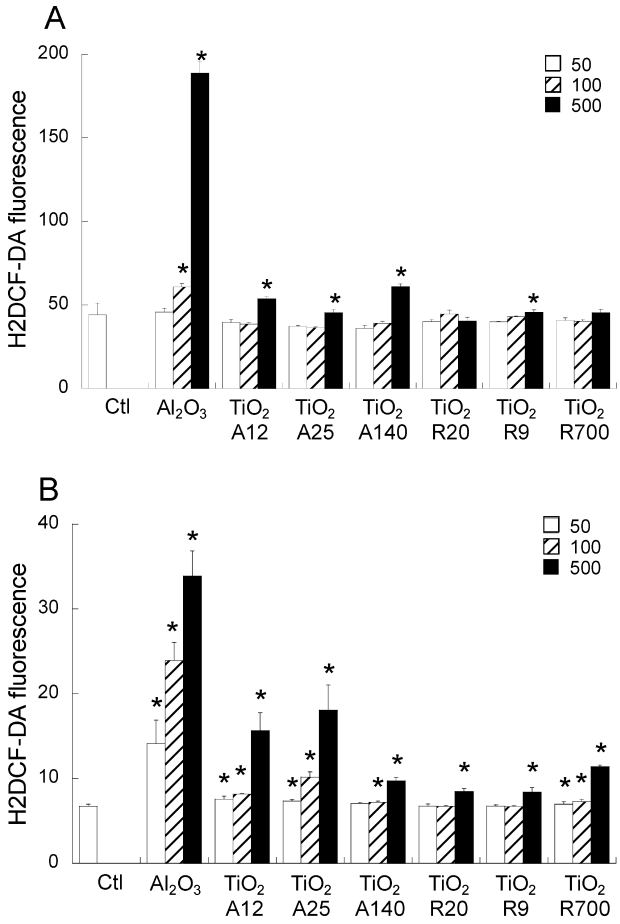


**FIGURE 6. ROS intracellular level. ROS formation was followed via monitoring the increasing fluorescence of H2DCF-DA. *E. coli* MG1655 (A) and *C. metallidurans* CH34 (B) were exposed for 2 h to 50, 100, 500 mg/L of $TiO_2$ or $Al_2O_3$ nanoparticles. ROS intracellular elevation was evaluated by comparison with ROS level in unexposed cells (Ctl). Statistical significance: *, $p < 0.05$.**

thus protecting plasma membrane. Another hypothesis for this resistance comes from the postulate that some products of genes located in *C. metallidurans* CH34 plasmids may play a role in maintaining the integrity of the cell wall, particularly in restoration of the outer membrane (*34*). Rather than being able to export nanoparticles, sensors in *C. metallidurans* CH34 periplasm may be activated and induce appropriate repair mechanisms, such as membrane restoration or oxidative stress counteraction.

**Effect of NP on Intracellular ROS Level.** To elucidate the dark mechanism of $TiO_2$ NP toxicity, the effect of NP exposure on cellular reactive oxygen species (ROS) level was probed using H2-DCF-DA staining (Figure 6). After 2 h of exposure to NP, $Al_2O_3$ induced a drastic increase in ROS intracellular level in both bacteria. The induction of ROS by $Al_2O_3$ NP may come from the presence of Al ions in NP suspension. Most of the $TiO_2$ NP induced an elevation of ROS level in both bacteria; the more oxidative NP were $TiO_2$-A12, -A25, and -A140, i.e., anatase NP. Nevertheless rutile NP also induced significant ROS production at the highest exposure concentration (500 mg/L). Still ROS intracellular level elevation was not very important. In *E. coli* MG1655, ROS production could not always be correlated to the observed loss of viability: $TiO_2$-A140 induced the production of ROS while it was not bactericidal. This suggests that even if NP caused oxidative stress in *E. coli* MG1655, this stress was not the only explanation for NP toxicity. We suggest that bacterial loss of viability is rather due to an impairment of membrane integrity. It is also the case in *C. metallidurans* CH34, since ROS production was induced by NP while no loss of viability was observed. Indeed, *C. metallidurans* CH34 kept a remarkable capacity to counteract the NP-generated oxidative stress, confirming that the resistance of this bacterium may be based on an overexpression of protecting components.

In this article was demonstrated that when nonagglomerated, $Al_2O_3$, $TiO_2$ NP and MWCNT are toxic to *E. coli* MG1655. The toxicity of $Al_2O_3$ NP could be partly explained by their dissolution. The more toxic $TiO_2$ NP, were the smallest (diameter <25 nm), round-shaped, with a neutral or positive zeta potential. When bactericidal, NP were always adsorbed onto bacterial surface and internalized in periplasm; however internalized NP were not always bactericidal: internalized in *C. metallidurans* CH34 they did not cause death. Bactericidal effects were partly due to NP-induced production of intracellular ROS, but we rather think that the impairment of cell membrane integrity is the major cause of bacterial death. The resistance of *C. metallidurans* CH34 may be related to its remarkable capacity to counteract the toxic action of NP, by overexpression of protective components such as oxidative stress or membrane restoration elements. Taken together, these data give valuable information on the mechanisms leading to NP-induced bacterial death. Still these experiments were performed on pure cultures, exposed to NP in pure water, i.e., a condition where bacteria are osmotically shocked. The impact of NP will surely be different in an environmental context, where bacterial cells are less numerous and exposure media also contain soil colloids which may adsorb or modify the physicochemical characteristics of NP. Finally this study was done on Gram-negative bacteria; more information is needed, on Gram-positive bacteria, to address the real risk associated to environmental exposure of bacteria to NP.

## Acknowledgments

This work received funding by ADEME (Agence de l'Environnement et de la Maitrise de l'Energie), French national research agency (ANR) and the Ile-de-France region in the framework of C'nano IdF. We thank Max Mergeay for the generous gift of *C. metallidurans* CH34 and D. Jaillard from CCME (Centre Commun de Microscopie Electronique d'Orsay, France) for helping with TEM sample preparation and observations.

## Supporting Information Available

Detailed protocols and a size distribution of dispersed MWCNT. This material is available free of charge via the Internet at http://pubs.acs.org.

## Literature Cited

(1) Adams, L. K.; Lyon, D. Y.; Alvarez, P. J. Comparative eco-toxicity of nanoscale $TiO_2$, $SiO_2$, and ZnO water suspensions. *Water Res.* **2006**, *40*, 3527–3532.

(2) Auffan, M.; Achouak, W.; Rose, J; Roncato, M. A; Chanéac, C.; Waite, D. T.; Masion, A. J. C. W.; Wiesner, M. R.; Bottero, J. Y. Relation between the redox state of iron-based nanoparticles and their cytotoxicity towards *Escherichia coli*. *Environ. Sci. Technol.* **2008**, *42*, 6730–6737.

(3) Brayner, R.; Ferrari-Iliou, R.; Brivois, N.; Djediat, S.; Benedetti, M. F.; Fievet, F. Toxicological impact studies based on Escherichia coli bacteria in ultrafine ZnO nanoparticles colloidal medium. *Nano Lett.* **2006**, *6*, 866–870.

(4) Heinlaan, M.; Ivask, A.; Blinova, I.; Dubourguier, H. C.; Kahru, A. Toxicity of nanosized and bulk ZnO, CuO, and $TiO_2$ to bacteria Vibrio fischeri and crustaceans Daphnia magna and Thamnocephalus platyurus. *Chemosphere.* **2008**, *71*, 1308–1316.

(5) Huang, Z.; Zheng, X.; Yan, D.; Yin, G.; Liao, X.; Kang, Y.; Yao, Y.; Huang, D.; Hao, B. Toxicological effect of ZnO nanoparticles based on bacteria. *Langmuir* **2008**, *24*, 4140–4144.

(6) Jiang, W.; Mashayekhi, H.; Xing, B. Bacterial toxicity comparison between nano- and micro-scaled oxide particles. *Environ. Pollut.* **2009**, *157*, 1619–1625.

(7) Jones, N.; Ray, B.; Ranjit, K. T.; Manna, A. C. Antibacterial activity of ZnO nanoparticle suspensions on a broad spectrum of microorganisms. *FEMS Microbiol. Lett.* **2008**, *279*, 71–76.
(8) Nair, S.; Sasidharan, A.; Divya Rani, V. V.; Menon, D.; Nair, S.; Manzoor, K.; Raina, S. Role of size scale of ZnO nanoparticles and microparticles on toxicity toward bacteria and osteoblast cancer cells. *J. Mater. Sci. Mater. Med.* 2008.
(9) Reddy, K. M.; Feris, K.; Bell, J.; Wingett, D. G.; Hanley, C.; Punnoose, A. Selective toxicity of zinc oxide nanoparticles to prokaryotic and eukaryotic systems. *Appl. Phys. Lett.* **2007**, *90*, 1–8.
(10) Sondi, I.; Salopek-Sondi, B. Silver nanoparticles as antimicrobial agent: a case study on E. coli as a model for Gram-negative bacteria. *J. Colloid Interface Sci.* **2004**, *275*, 177–182.
(11) Stoimenov, P. K.; Klinger, R. L.; Marchin, G. L.; Klabunde, K. J. Metal oxide nanoparticles as bactericidal agents. *Langmuir* **2002**, *18*, 6679–6686.
(12) Thill, A.; Zeyons, O.; Spalla, O.; Chauvat, F.; Rose, J.; Auffan, M.; Flank, A. M. Cytotoxicity of $CeO_2$ nanoparticles for *Escherichia coli*. Physico-chemical insight of the cytotoxicity mechanism. *Environ. Sci. Technol.* **2006**, *40*, 6151–6156.
(13) Chithrani, B. D.; Ghazani, A. A.; Chan, W. C. W. Determining the size and shape dependence of gold nanoparticle uptake into mammalian cells. *Nano Lett.* **2006**, *6*, 662–668.
(14) Lok, C. N.; Ho, C. M.; Chen, R.; He, Q. Y.; Yu, W. Y.; Sun, H.; Tam, P. K. H.; Chiu, J. F.; Che, C. M. Silver nanoparticles: partial oxidation and antibacterial properties. *J. Biol. Inorg. Chem.* **2007**, *12*, 527–534.
(15) Pal, S.; Tak, Y. K.; Song, J. M. Does the antibacterial activity of silver nanoparticles depend upon the shape of the nanoparticle? A study of the Gram negative *Escherichia coli*. *Appl. Environ. Microbiol.* **2007**, *73*, 1712–1720.
(16) Kang, S.; Herzberg, M.; Rodrigues, D. F.; Elimelech, M. Antibacterial effects of carbon nanotubes: size does matter. *Langmuir* **2008**, *24*, 6409–6413.
(17) Upadhyayula, V. K.; Deng, S.; Mitchell, M. C.; Smith, G. B.; Nair, V. K.; Ghoshrov, S. Adsorption kinetics of Escherichia coli and Staphylococcus aureus on single-walled carbon nanotube aggregates. *Water Sci. Technol.* **2008**, *58*, 179–184.
(18) Upadhyayula, V. K.; Deng, S.; Smith, G. B.; Mitchell, M. C. Adsorption of *Bacillus subtilis* on single-walled carbon nanotube aggregates, activated carbon and NanoCeram. *Water Res.* **2009**, *43*, 148–156.
(19) Pulskamp, K.; Diabate, S.; Krug, H. F. Carbon nanotubes show no sign of acute toxicity but induce intracellular reactive oxygen species in dependence on contaminants. *Toxicol. Lett.* **2007**, *168*, 58–74.
(20) Mergeay, M.; Nies, D.; Schlegel, H. G.; Gerits, J.; Charles, P.; Vangijsegem, F. Alcaligenes eutrophus CH34 is a facultative chemolithotroph with plasmid-bound resistance to heavy metals. *J. Bacteriol.* **1985**, *162*, 328–334.
(21) Mergeay, M. *Bacteria Adapted to Industrial Biotopes: Metal-Resistant Ralstonia*; American society for microbiology: Washington, DC, 2000.
(22) Pinault, M.; Mayne-L'Hermite, M.; Reynaud, C.; Pichot, V.; Launois, P.; Ballutaud, D. Growth of multiwalled carbon nanotubes during the initial stages of aerosol-assisted CCVD. *Carbon.* **20042005**, *43*, 2968–2976.
(23) Pinault, M.; Mayne-L'Hermite, M.; Reynaud, C.; Beyssac, O.; Rouzaud, J. N.; Clinard, C. Carbon nanotubes produced by aerosol pyrolysis: growth mechanisms and post-annealing effects. *Diamond Relat. Mater.* **2004**, *13*, 1266–1269.
(24) Pignon, B.; Maskrot, H.; Leconte, Y.; Coste, S.; Reynaud, C.; Herlin-Boime, N.; Gervais, M.; Guyot Ferreol, V.; Pouget, T.; Tranchant, J. F. Versatility of laser pyrolysis applied to synthesis of $TiO_2$ nanoparticles, application to UV attenuation. *Eur. J. Inog. Chem.* **2008**, *6*, 883–889.
(25) Simon-Deckers, A.; Gouget, B.; Mayne-L'hermite, M.; Herlin-Boime, N.; Reynaud, C.; Carriere, M. In vitro investigation of oxide nanoparticle and carbon nanotube toxicity and intracellular accumulation in A549 human pneumocytes. *Toxicology* **2008**, *253*, 137–146.
(26) Brunauer, S.; Emmett, P. H.; Teller, E. Adsorption of gases in multimolecular layers. *J. Am. Chem. Soc.* **1938**, *60*, 309–319.
(27) Blattner, F. R.; Plunkett, G.; Bloch, C. A.; Perna, N. T.; Burland, V.; Riley, M.; ColladoVides, J.; Glasner, J. D.; Rode, C. K.; Mayhew, G. F.; Gregor, J.; Davis, N. W.; Kirkpatrick, H. A.; Goeden, M. A.; Rose, D. J.; Mau, B.; Shao, Y. The complete genome sequence of *Escherichia coli* K-12. *Science* **1997**, *277*, 1453–1474.
(28) Maness, P. C.; Smolinski, S.; Blake, D. M.; Huang, Z.; Wolfrum, E. J.; Jacoby, W. A. Bactericidal activity of photocatalytic TiO(2) reaction: toward an understanding of its killing mechanism. *Appl. Environ. Microbiol.* **1999**, *65*, 4094–4098.
(29) Kang, S.; Mauter, M. S.; Elimelech, M. Physicochemical determinants of multiwalled carbon nanotube bacterial cytotoxicity. *Environ. Sci. Technol.* **2008**, *42*, 7528–7534.
(30) Kang, S.; Pinault, M.; Pfefferle, L. D.; Elimelech, M. Single-walled carbon nanotubes exhibit strong antimicrobial activity. *Langmuir* **2007**, *23*, 8670–8673.
(31) Monthioux, M.; Smith, B. W.; Burteaux, B.; Claye, A.; Fischer, J. E.; Luzzi, D. E. Sensitivity of single-wall carbon nanotubes to chemical processing: an electron microscopy investigation. *Carbon* **2001**, *39*, 1251–1272.
(32) von Rozycki, T.; Nies, D. *Cupriavidus metallidurans*: Evolution of a metal-resistant bacterium. *Antonie van Leeuwenhoek* **2009**, *96*, 115–139.
(33) Vollmer, W.; Blanot, D.; de Pedro, M. A. Peptidoglycan structure and architecture. *FEMS Microbiol. Rev.* **2008**, *32*, 149–167.
(34) Monchy, S.; Benotmane, M. A.; Janssen, P.; Vallaeys, T.; Taghavi, S.; Van der Lelie, D.; Mergeay, M. Plasmids pMOL28 and pMOL30 of *Cupriavidus metallidurans* are specialized in the maximal viable response to heavy metals. *J. Bacteriol.* **2007**, *189*, 7417–7425.

ES9016975